t -

Presented at IEEE Conference on Robotics and Automation
Philadelphia, April, 1988

Superquadric Artificial Potentials for Obstacle Avoidance and Approach

Pradeep Khosla
Department of Electrical and Computer Engineering

Richard Volpe
Department of Physics

Carnegie-Mellon University
Pittsburgh. Pennsylvania 15213

Abstract

Previous use of artificial potentials has demonstrated the need for an obstacle avoidance potential that closely models he obstacle. yet does not generate local minima in the workspace of the manipulator. Recently we proposed a new elliptical potential function which satisfies these requirements for rectangular objects in spherically symmetric attractive wells. In this paper we present a new obstacle avoidance potential based on superquadrics. The superquadric formulation is a generalization of the elliptical potential function method, and therefore is viable for a much larger class of object shapes. As with elliptical potentials, a modified form of he superquadric potential provides safe approach toward objects. We have implemented the avoidance and approach potentials in simulations and the results exhibit an improvement over existing potential schemes. The simulations also employ an algorithm that eliminates collisions with obstacles by calculating the repulsive forces exerted on links, based on the shortest distance to an object.

1 Introduction

An artificial potential is a mathematical description of the potential energy within the workspace of a manipulator. Regions in the workspace that are to be avoided are modelled by repulsive potentials (energy peaks), and the region to which the end effector is to move is modelled by an attractive potential (energy valley). The addition of repulsive and attractive potentials provides the desired workspace energy topology. Thus, for each point in the real workspace of the manipulator there is a modelled value of potential energy and an associated gradient or force. This force causes the end effector of the manipulator to move through its environment in a manner which is directly responsive to the modelled potential energy function of that environment.

The major interest in artificial potential models has been in realizing obstacle avoidance schemes [10,12,11,13,8,14]. In an unobstructed environment, a simple bowl-shaped attractive potential will drive the manipulator to its center. But this potential will not suffice in an obstructed environment. Repulsive potential hills must be added to the attractive potential at the locations of obstacles, as in Figure 1. The addition of repulsive potentials provides obstacle avoidance capability.

But the addition of attractive and repulsive potentials can expose a major problem with artificial potentials: the presence of local minima in the potential function. Any local minimum can cause the manipulator to experience no net artificial force, and thereby stop at an unintended location. A robust artificial potential model of the environment will have no local minima [11,14].

We have proposed a second use of artificial potentials — obstacle approach [14]. Instead of having a potential function go to infinity at the object surface (as with the avoidance potential), the potential can go smoothly to a finite value. As the manipulator moves toward the object, it gains potential energy, loses kinetic energy, and slows down. Thus the approach potential determines the necessary deceleration forces that will provide a safe contact velocity at the surface.

Previously, we have presented a elliptical potential function that can be used for both obstacle avoidance and object approach. This function is useful for rectangular objects. In this paper we present a superquadric formulation for use with more general object shapes [3,2]. First, however, the history of the potential approach is outlined, and some of the problems indicated. Then, our new potential function is described and its advantages are highlighted. Finally, the developed potential is employed in simulations of two and three link manipulators.

Currently, the proposed artificial potential scheme is being experimentally implemented and evaluated on the CMU DD ARM II.

2 Attributes of Artificial Potentials

As was stated earlier, potentials may be divided into two types: attractive and repulsive potentials.

Attractive potentials are generally quadratic wells [9,7,11]. As we have outlined previously, quadratic wells are beneficial for two reasons [14]. First, a quadratic well provides a linear control law with constant gain; and second, all stablizing potentials are quadratic for small displacements.

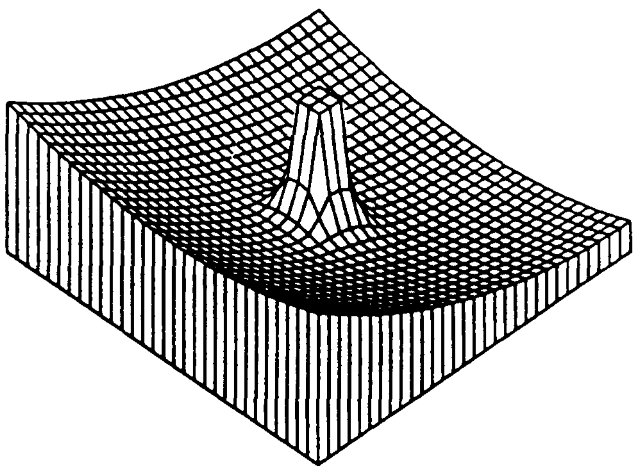

Figure 1: A repulsive potential added to an attractive well.

A conical well has also been proposed [1]. It is quadratic to a given range and then increases linearly:

$$U(\mathbf{x}) = \begin{cases} l\mathbf{x} \cdot \mathbf{x}, & |\mathbf{x}| < 1 \\ 2l|\mathbf{x}| - l, & |\mathbf{x}| \geq 1 \end{cases} \tag{1}$$

where l is a constant and $\mathbf{x}$ is the position vector. This conical well provides a constant magnitude, centrally attractive, force field for large distances. While, for small distances, the stability of a quadratic well is utilized.

The second category of potentials, repulsive potentials, are necessary to repel the manipulator away from obstacles that obstruct its path of motion to the global attractive well. It has generally been recognized that a repulsive potential should have a limited range of influence [1,9]. This prevents an object from affecting the motion of the manipulator when it is far away from the object. Also, the potential function and its derivative must change smoothly and never become discontinuous [1].

Many proposed repulsive potentials have spherical symmetry. One increases cubically with radial distance inside of a circular threshold range [1]. Another has a Gaussian shape [11]. These potentials are useful for surrounding objects with spherical symmetry and singularities in the workspace. Also, when added to a spherically symmetric attractive well they will not create a local minimum (as will be demonstrated subsequently). But a spherically symmetric repulsive potential does not follow the contour of polyhedral objects. For instance, an oblong object surrounded by a sphere effectively eliminates much more volume from the workspace than is necessary or desirable.

The FIRAS function was proposed to address the insufficiency of radially symmetric potentials [9]. The potential energy, $U(r)$, of the FIRAS function is described by:

$$U(r) = \frac{A}{2}\left(\frac{1}{r} - \frac{1}{r_0}\right)^2 \qquad 0 < r < r_0 \tag{2}$$

where r is the closest distance to the object surface, r_0 is the effective range, and A is a scaling factor. Figure 2 shows this potential for $A = 2$ and $r_0 = 6$. The isopotential contours of this potential function are depicted in Figure 3.

By itself the FIRAS potential works well. But when this potential is added to an attractive well, local minima appear on the side of the object away from the center of the well. Consider the case depicted in Figure 4, where the side of the object away from the attractive well center is tangent to the isopotential contours of the well. Motion along the linear section of the object contour, from point A to point B, passes through changing potential values of the attractive well. At A and B the attractive well potential is higher than at point C. Since the object potential is the same at A, B, and C, the sum of the object potential and the attractive well potential has a local minimum at point C. It can be seen that any section of an object contour that has a radius of curvature greater than that of the attractive well will generate a local minimum 'uphill' from the object. A circular repulsive potential always has a smaller radius of curvature than the attractive well in which it is inscribed. Therefore, a circular repulsive potential will not generate local minima in this way.

In summary, a potential function that is useful for modelling objects in the environment should have the following attributes:

1. The potential should have spherical symmetry for large distances to avoid the creation of local minima when this potential is added to others.

2. The potential contours near the surface should follow the surface contour so that large portions of the workspace are not effectively eliminated.

3. The potential of an obstacle should have a limited range of influence.

4. The potential and the gradient of the potential must be continuous.

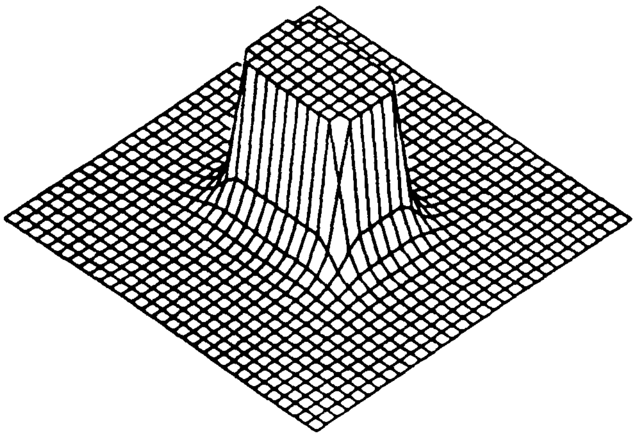

Figure 2: The FIRAS potential for $A = 2$ and $r_0 = 6$. Large values have been truncated.

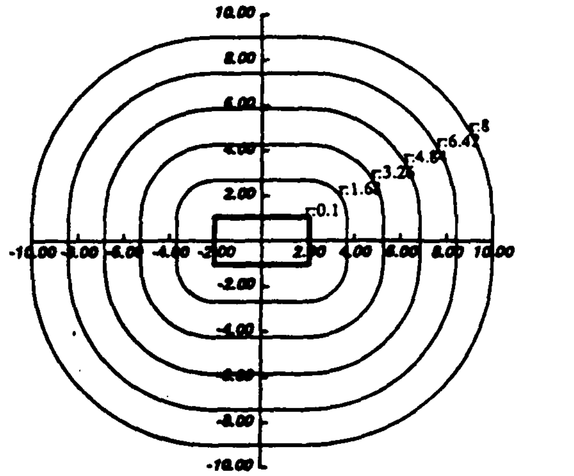

Figure 3: The isopotential contours of the FIRAS potential in Figure 2.

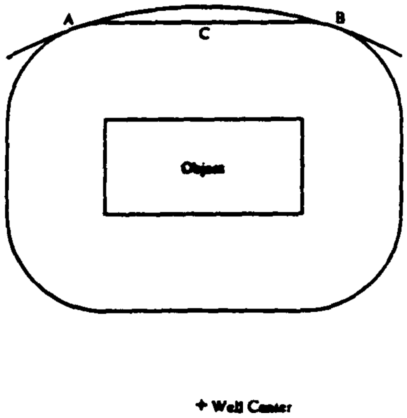

Figure 4: The coincidence of isopotential contours at points A and B indicates the presence of a local minimum in the vicinity of point C.

3 Superquadric Potentials

3.1 Superquadric Avoidance Potentials

To avoid the creation of minima the object potential must be spherical, as described in criterion number one. However, a potential that is spherical at all distances will not work for nonspherical objects. In this section, we present a potential function which changes from the object shape near the object, to spherical away from it (*circular* in two dimensions), and satisfies the four outlined criteria.

3.1.1 Superquadric Isopotential Contours

The shape of a potential function is described by its isopotential contours. Therefore, criteria one and two must be satisfied by the creation of appropriate isopotential contours for the potential function.

To satisfy the second criterion, an object may be surrounded with a superquadric [3,2]:

$$\left[\left(\frac{x}{f_1(x,y,z)}\right)^{2n} + \left(\frac{y}{f_2(x,y,z)}\right)^{2n}\right]^{\frac{m}{n}} + \left(\frac{z}{f_3(x,y,z)}\right)^{2m} = 1 \qquad (3)$$

where f_1, f_2, and f_3 are scaling functions, and m and n are exponential parameters. Previously we have employed this function in two dimensions ($z = 0$) with constant scaling functions [14]:

$$\left(\frac{x}{a}\right)^{2n} + \left(\frac{y}{b}\right)^{2n} = 1. \qquad (4)$$

This form is called an n-ellipse where a is the semi-major axis and b is the semi-minor axis [6,9]. It is valuable to review the use of this simpler form in potential functions and then show how it may be generalized to the superquadric potential form.

In order for the above n-ellipse to be useful as a potential function, two constraints should be imposed at the surface of the object: first, the ellipse must touch the corners of the surrounded object (which is rectangular for this case); and second, the area between the object and the ellipse must be minimal. These constraints yield:

$$a = \frac{w}{2}\left(2^{\frac{1}{2n}}\right) \qquad b = \frac{h}{2}\left(2^{\frac{1}{2n}}\right) \qquad (5)$$

where w is the x dimension of the rectangle, and h is the y dimension.

At the surface of the object, the isopotential contours should match the shape of the surface. This requires that n go to infinity at the surface. However, away from the surface the contours must become spherical in order to satisfy the first criterion. Letting n go to one will make the contours elliptical. This ellipse may be further modified by a coefficient that multiplies the y term. The contour function thus becomes:

$$\left(\frac{x}{a}\right)^{2n} + \left(\frac{b}{a}\right)^2\left(\frac{y}{b}\right)^{2n} = 1 \qquad n \geq 1. \qquad (6)$$

It is also necessary to have a variable that specifies each contour. This variable should act as a pseudo-distance from the object, being zero at the surface and increasing with successive contours away from the surface. Along the x axis this variable can be made to change linearly. Thus,

$$K = \left[\left(\frac{x}{a}\right)^{2n} + \left(\frac{b}{a}\right)^2\left(\frac{y}{b}\right)^{2n}\right]^{\frac{1}{2n}} - 1. \qquad (7)$$

Figure 5 shows a plot of K at regular intervals with n varying from a very large value to a value near unity.

Since the parameter n must vary from infinity to one while K varies from zero to infinity, n has been defined as:

$$n = \frac{1}{1 - e^{-\alpha\beta_n K}} \qquad (8)$$

Figure 5: The isopotential contours for $K = 0.1$ to $K = 2.6$, and $\alpha = 1.5$.

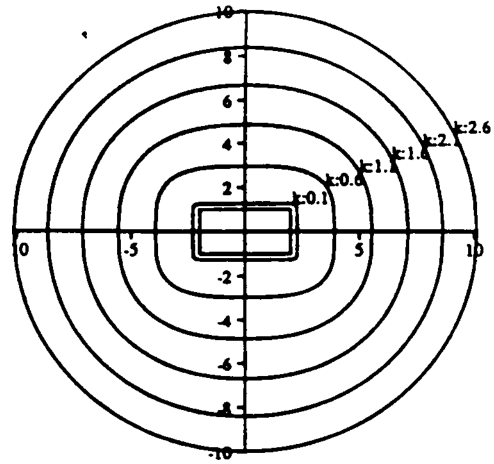

Figure 6: Superquadric isopotential contours for a trapezoid

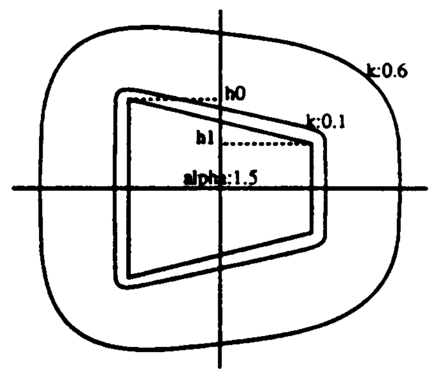

where α and β_n are adjustable parameters. Unless otherwise noted, β_n will be unity. Other definitions of n are possible, but this form is valuable because it is related to the magnitude of the potential, as will be shown in Section 3.1.2.

The above description, expanded to three dimensions, can yield an ellipsoid instead of an ellipse. For the three dimensional case, f_3 in Equation (3) is a third constant semi-axis, c, and the parameter m can be given the form:

$$m = \frac{1}{1 - e^{-\alpha\beta_m K}}. \qquad (9)$$

If the parameter β_m is set equal to β_n, then m equals n and Equation (3) is an n-ellipsoid.

The elliptical (ellipsoidal) description may be generalized to the superquadric formulation by using nonconstant scaling functions, f_i, in Equation (3). This provides a method of deforming the n-ellipse (ellipsoid) to other shapes. This effect can be understood as changing the semi-axes of the ellipse (ellipsoid). An example can be shown in two dimensions for a superquadric contour that snugly surrounds a trapezoid as in Figure 6. In this case, the semi-minor axis b must vary from b_0 to b_1 as the height of the object varies from h_0 to h_1. Therefore, at the object surface ($K = 0$),

$$b(x) = mx + d \qquad (10)$$

$$m = \frac{h_1 - h_0}{2w} = \frac{b_1 - b_0}{2a} \qquad (11)$$

$$d = \frac{b_1 + b_0}{2} \qquad (12)$$

Figure 7: The isopotential contours surrounding a triangle for $K = 0.1$ to $K = 2.6$, and $\alpha = 1.5$.

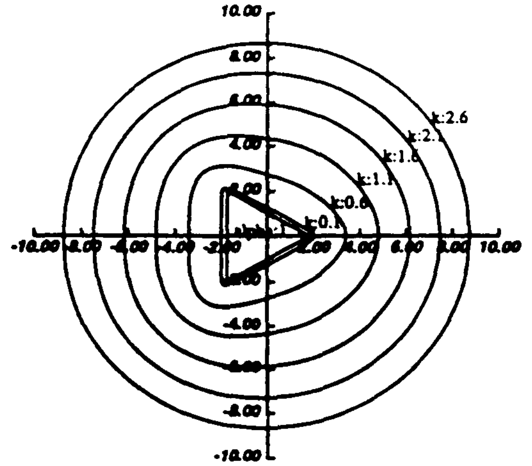

Figure 8: The avoidance potential for a triangle with $\alpha = 1$ and $A = 1$. Large values have been truncated.

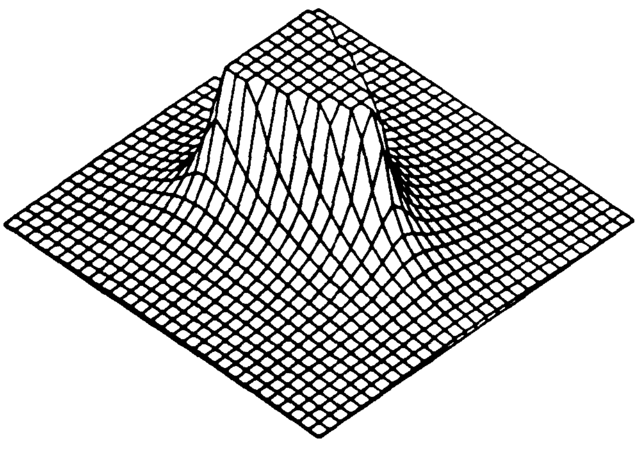

This value of b provides a superquadric which touches the corners of the trapezoid, with $K = 0$. Superquadric isopotential contours away from the object may be obtained by scaling x:

$$f_2 = m\frac{x}{K+1} + d. \tag{13}$$

Reducing h_1 to a very small value gives a superquadric model of a triangle, as shown in Figure 7.

Finally, this example can be extended into three dimensions for superquadric models of wedges, pyramids, and cones. For a wedge,

$$f_1 = a \tag{14}$$

$$f_2 = m\frac{x}{K+1} + d \tag{15}$$

$$f_3 = c. \tag{16}$$

For a pyramid,

$$f_1 = a \tag{17}$$

$$f_2 = m_2\frac{x}{K+1} + d_2 \tag{18}$$

$$f_3 = m_3\frac{x}{K+1} + d_3. \tag{19}$$

And for a cone oriented along the z-axis,

$$n = 1 \tag{20}$$

$$f_1 = m\frac{z}{K+1} + d \tag{21}$$

$$f_2 = m\frac{z}{K+1} + d \tag{22}$$

$$f_3 = c. \tag{23}$$

3.1.2 Avoidance Potential

With the form of the isopotential contours established, it is necessary to assign potential energy values to them. These energy values must satisfy the third and fourth criteria outlined in Section 2, and in accordance with natural potentials (e.g. electrostatic, gravitational, etc.) exhibit an inverse dependence on distance. Therefore, the potential function must have a K^{-1} dependence for short distance repulsion, but drop to zero faster than K^{-1} for large distances. Also, the function and its derivative must be continuous. A function that satisfies these criteria is the Yukawa potential [5]:

$$U(K) = A\frac{e^{-\alpha K}}{K} \tag{24}$$

Figure 8 shows this function with $\alpha = 1$ and $A = 1$ for a triangle.

The parameter α determines how rapidly the potential rises near the object and falls off away from the object. Therefore, this parameter must also appear in Equation (8), which determines how quickly the 'n-ness' of the ellipse changes to accommodate the change in the magnitude of the potential. The parameter A acts as an overall scale factor for the potential. Large values of A will make the object have a spherical field of repulsive force at large distances. Small values of A will allow the object to be approached much more closely. At this closer range, the isopotential contours will have large values of n and will approximate the shape of the object. For the rest of this discussion A will assumed to be unity unless otherwise noted.

3.2 Superquadric Approach Potentials

The attractive potential has already been discussed as one method of moving the manipulator to a desired point. This strategy, however, requires damping of the arm to prevent oscillation about the destination point. In effect, the damping is required to absorb the kinetic energy that the arm attains by moving from its starting point of higher potential energy. An alternative way of absorbing the energy is to increase the the potential energy of its destination. Thus, the arm moves 'downhill' from its starting point and then 'uphill' to its destination.

An appropriate approach potential should follow all of the criteria of the avoidance potential, but should go to a finite maximum value at the surface of the object. Therefore, far from the object, the form of the avoidance potential may be used. However, closer to the surface the potential should be Gaussian in nature, the slope smoothly changing to zero at the surface so that no artificial force is experienced when real contact with the environment is established. Because this general form must remain for all values of α, a simple polynomial fit is not possible. A function which does satisfy these criteria is:

$$U(K) = \begin{cases} \frac{A}{K}e^{-\alpha K}, & K \geq 1 \\ A\exp\left(-\alpha K^{1+\frac{1}{\alpha}}\right), & 1 > K \geq 0 \end{cases} \tag{25}$$

Figure 9 shows this function with $\alpha = 1$ for a triangle.

Figure 9: The approach potential function for a triangle with $\alpha = 1$.

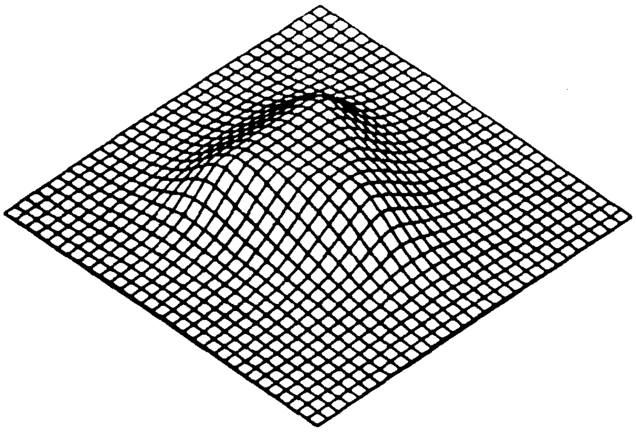

4 Addition of a Superquadric Avoidance Potential and an Attractive Well

The concern when adding an avoidance potential to an attractive well, is that an undesirable minimum may be created 'uphill' from the object. Because the superquadric avoidance potential only becomes a circle asymptotically, a spurious minimum may be present. However, this minimum can effectively be removed by making the depression associated with it smaller than the resolution of the system.

For a rectangular object, the minimum value of α is determined for its worst case orientation. This is when the longest dimension of the object to be avoided is tangent to the isopotential contours of the attractive well. In other words, the object is placed 'across' the desired path. We have previously shown that a local minimum caused by this orientation in a quadratic well may be easily removed by adjusting the parameter α [14].

For a rectangular object in the conical well, a similar analysis may be performed. Using a coordinate system centered on the object, with the x axis along its longest dimension, yields:

$$U = U_o(K) + U_w(\mathbf{x}) \tag{26}$$

with the object and well potentials given by:

$$U_o = \frac{e^{-\alpha K}}{K} \quad \text{and} \quad U_w = 2l|\mathbf{x}| - l \tag{27}$$

with l constant and $\mathbf{x} = (x, y - y_0)$, where y_0 is the location of the attractive well center.

First it is necessary to find the local minimum along the y axis that is on the opposite side of the object from the attractive well center. At this point the total force is zero.

$$0 = \nabla U = \frac{\partial}{\partial x}[U_o + U_w]\hat{x} + \frac{\partial}{\partial y}[U_o + U_w]\hat{y} \tag{28}$$

or

$$0 = \frac{\partial U}{\partial K}\left[\left(\frac{x}{a}\right)^{2n} + \left(\frac{b}{a}\right)^2\left(\frac{y}{b}\right)^{2n}\right]^{\frac{1}{2n}-1}\left(\frac{1}{a}\right)^{2n} x^{2n-1} + \frac{2lx}{|\mathbf{x}|} \tag{29}$$

$$0 = \frac{\partial U}{\partial K}\left[\left(\frac{x}{a}\right)^{2n} + \left(\frac{b}{a}\right)^2\left(\frac{y}{b}\right)^{2n}\right]^{\frac{1}{2n}-1}\frac{b^{2-2n}}{a^2} y^{2n-1} + \frac{2l(y - y_0)}{|\mathbf{x}|} \tag{30}$$

where

$$\frac{\partial U}{\partial K} = -e^{-\alpha K}\left[\frac{\alpha}{K} + \frac{1}{K^2}\right] \tag{31}$$

Considering only the y direction,

$$\left.\frac{\partial U}{\partial y}\right|_{x=0} = \frac{\partial U}{\partial K}\left[\left(\frac{b}{a}\right)^2\left(\frac{y}{b}\right)^{2n}\right]^{\frac{1}{2n}-1}\left(\frac{b}{a}\right)^2\left(\frac{1}{b}\right)^{2n} y^{2n-1} + 2l \tag{32}$$

is a quadratic equation of the form:

$$0 = -e^{-\sigma}(\sigma + 1)c + 2l(cy - 1)^2. \tag{33}$$

with

$$K(x=0) = cy - 1, \qquad c \equiv \left(\frac{b}{a}\right)^{\frac{1}{n}}\left(\frac{1}{b}\right), \qquad \sigma \equiv \alpha K \tag{34}$$

Solving for the meaningful root of this equation yields:

$$y = \frac{1}{c} + \sqrt{\frac{e^{-\sigma}(\sigma + 1)}{2lc}} \tag{35}$$

Having solved for the y coordinate of the minimum. it is necessary to determine the size of rk local depression. This is done by finding the first maximum in the x direction for rk given value ofy. From Equations 29 rad 30.

$$x = \frac{a}{b}\left[\frac{y^{2n-1}}{y - y_0}\right]^{*} \tag{36}$$

Given that the resolution of the system being modelled must be less than $2x$, it is only necessary to satisfy the above equation. Because y and n are both functions of σ, this equation can be used for an iterative solution of σ. With a value of σ determined, y and n may be obtained, followed by K and α. In this way, a minimum value of α may be calculated which permits the addition of a conical attractive well and the repulsive superquadric potential for a rectangular object, without the creation of a local minimum.

For non-rectangular objects in quadratic and conical wells, the same analyses may be used. The rectangle considered has the dimensions of the maximum height and width of the non-rectangular object. A valid bound for α is determined since the rectangle is more likely to form a local minima. This is because the superquadric isopotential contours that intersect the object axes at right angles have an infinite radius of curvature at the points of intersection. That is, the contour is straight at these points. For example, the contours surrounding a square have an infinite radius of curvature at the x and y axes. Therefore, a local minimum may occur for the same reason that was outlined earlier for the FIRAS potential. The parameter α eliminates this minimum by forcing the isopotential contours to circles at the range of the former minimum. The value of α that is large enough to make the contours sufficiently circular at the axes, will be large enough to make the contours circular in general. For a non-rectangular object the same value of α will also provide circular isopotential contours at the necessary range, ensuring that these objects will not cause local minima.

5 Simulation

To test these concepts the performance of two and three link planar manipulators interacting with an artificial potential have been simulated. The motion of these arms is caused by the artificial forces acting on the end effector and the individual links. The end effector is attracted by a goal *point* and repelled by the obstacle, while the links are repelled by the obstacle if the link interaction is 'on'. The results indicate that the superquadric potentials provide a valid method of obstacle avoidance for a manipulator, and an improvement over existing potential functions.

5.1 End Effector Interaction

There are two ways for the arm to react to the artificial forces applied to the end effector. The first method transforms the forces into the corresponding joint torques through the transpose of the Jacobian: $\tau = J^T F$. The joint accelerations can then be derived from the Lagrangian [4]. The second method obtains joint accelerations by directly transforming the Cartesian accelerations that would be experienced by a unit mass in the potential well: $\ddot{\theta} = J^{-1}\left(\ddot{x} - \dot{J}\dot{\theta}\right)$. The first method is desirable because it does not involve the inverse of the Jacobian, which may become singular. For avoidance potentials, the first method is used. But for reasons we have previously outlined, the second method must be used when employing an approach potential [14].

5.2 Link Interaction

While the end effector interaction with the artificial potentials will guide the end effector around obstacles, it will not prevent collisions of the links with the obstacles. To prevent these collisions, there must be an interaction of the links with the artificial force field. But the link occupies a region near the obstacles, not just a point. How then should the interaction be calculated? It would be too computationally intensive to integrate the total interaction of the link with the field. Also, it is the avoidance of collision that is of primary importance. Therefore, the point on the link which is closest to the obstacle should determine the amount of repulsion experienced. We have previously presented an algorithm which determines the point on a link which is closest to an obstacle [14]. The force due to the object is applied to the link at this point and the resultant motion is determined by the dynamics of the arm.

5.3 Simulation Experiments

Three main situations were examined: 1.) Unsuccessful acquisition of the goal while avoiding an object surrounded by the FIRAS potential, 2.) Movement to a goal point while avoiding an object surrounded by the proposed superquadric avoidance potential, 3.) and approach of an object surrounded by the proposed superquadric approach potential. In the first two situations the end effector experiences an attractive force from a goal point and a repulsive force from the obstacle, and the links of the arm experience a repulsive force from the obstacle. For the third situation, the use of a goal point is optional and there is no link interaction.

5.3.1 FIRAS Potential

For many situations, the FIRAS potential provides a viable method of obstacle avoidance and goal acquisition. However, as was shown earlier, local minima can be created when the FIRAS potential is added to a circularly symmetric well [14]. When link interaction forces are not great enough to drive the end effector out of this minima, the arm will stop 'uphill' of the object. Figure 10 shows such a situation.

5.3.2 Superquadric Avoidance Potential

The same arm trajectory has been initiated with the superquadric potential in the circular attractive well. Figure 11 shows the end effector of a two link manipulator successfully navigating around the obstacle. This confirms the absence of a local minimum 'uphill' from the object. However, with only two degrees of freedom, the arm can not move completely around the obstacle — it becomes stuck when the repulsive torque of the obstacle on the second link equals the attractive torque of the goal point on the end effector. This is not a deficiency in the form of the potential, but a deficiency in the two link manipulator. Figure 12 shows that a three link design does not have this same problem. The arm is able to 'snake' around the obstacle, and the end effector is able to achieve the goal point.

A third situation was also examined. Four obstacles surrounded by superquadric avoidance potentials were placed in a conical attractive well. Figures 13 and 14 show the manipulator successfully navigating between them to achieve the specified goal point. The start and finish points were interchanged for the two simulations. Different trajectories were created, but the traversal time was about the same.

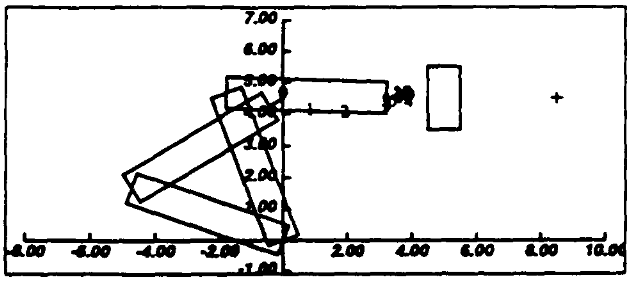

Figure 10: Unsuccessful avoidance of an obstacle using the FIRAS potential ($r_0 = 1.5$). The end effector has settled in a local minimum just 'uphill' from the obstacle.

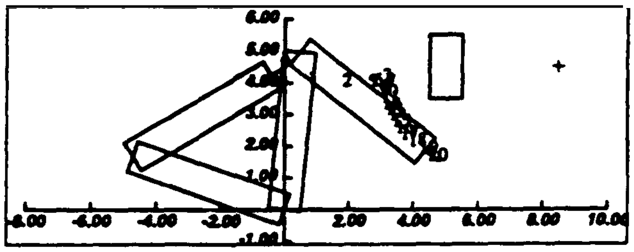

Figure 11: Successful avoidance of an obstacle using the newly proposed function. The minimum value of α that will allow avoidance has been used ($\alpha = 4.4$). The arm is prevented from reaching the goal by its geometric limitations.

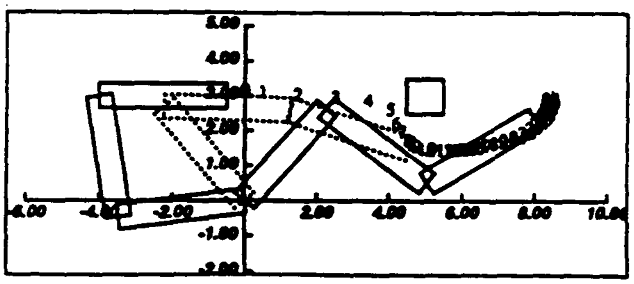

Figure 12: Successful avoidance of an obstacle using the newly proposed function. The minimum value of α that will allow avoidance has been used ($\alpha = 3.76$). The redundancy of the manipulator enables it to 'snake' its way around the obstacle. The dotted manipulator is an intermediate configuration.

Figure 13: Successful navigation around four obstacles using superquadric avoidance potentials and a modified conical attractive well. The dotted manipulators are intermediate configurations.

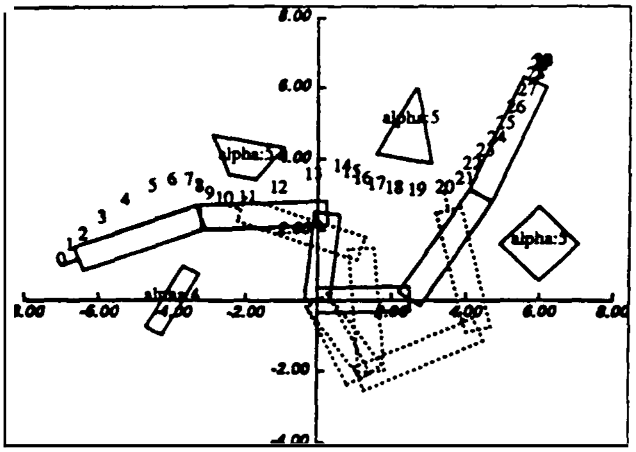

Figure 14: The same situation as Figure 13 except that the starting and ending points have been interchanged. Notice that a different trajectory has been created but the time of traversal is about the same.

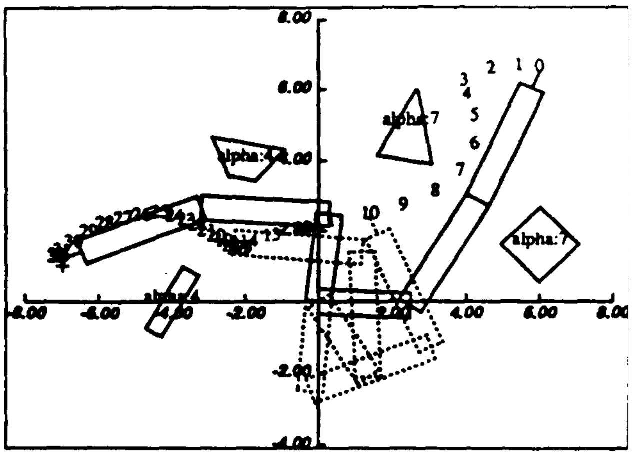

5.3.3 Approach Potential

Finally, the motion of the end effector approaching the surface of the object has been simulated in Figure 15. For this simulation, no attractive point was used. Instead, the arm was given an initial end effector velocity with its corresponding kinetic energy. The height of the potential at the surface was set to ninety percent of the initial kinetic and potential energy. To eliminate any computational errors due to the discrete time nature of the calculations, the height the potential was continually modified to ninety percent of the kinetic and potential energy. Also, the end effector was position controlled in the y direction.

Figure 15: This Figure shows successful approach and contact with an object surrounded by the proposed approach potential. For this simulation there was no attractive point, but the end effector was position controlled in the y direction. The initial velocity was 1 unit/sec in the x direction. The contact velocity was 0.06 unit/sec.

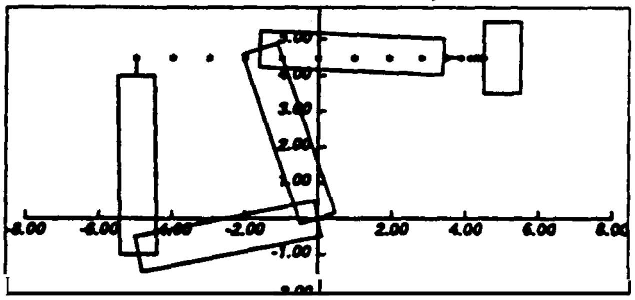

6 Summary

A new superquadric potential has been developed that improves upon previous artificial potentials by providing avoidance of obstacles without the generation of local minima. Also, since the contours of objects are followed, a modified version of the function may be used for object approach. These potentials have been implemented in simulations of two and three link manipulators. The results indicate an improvement over other potential schemes.

7 Acknowledgements

We would like to thank Professor Takeo Kanade for suggesting the use of superquadrics as a generalization of the n-ellipse formulation. We would also like to thank him for providing the necessary laboratory and computational facilities to conduct this work. This research is supported in part by an AFOSR graduate fellowship (for Richard Volpe) and the Department of Electrical and Computer Engineering.

References

[1] J. R. Andrews and N. Hogan. *Impedance Control As A Framework For Implementing Obstacle Avoidance In A Manipulator*, pages 243–251. ASME, 1983.

[2] A.H. Barr. Superquadrics and angle-preserving transformations. *IEEE Computer Graphics and Applications*, 1:11–23, 1981.

[3] R. Bajcsy and F. Solina. Three dimensional object representation revisited. In *First International Conference on Computer Vision*, pages 231–240, London, England, June 8-11 1987.

[4] M. Brady and et al. (editors). *Robot Motion: Planning and Control*. MIT Press, Cambridge, MA, 1982.

[5] B. Cohen-Tannoudji, C. Diu, and F. Laloe. *Quantum Mechanics*. Volume 2, John Wiley and Sons, New York, 1977.

[6] M. Gardner. The superellipse: a curve that lies between the ellipse and the rectangle. *Scientific American*, September 1965.

[7] H. Hanafusa and H. Asada. Stable prehension by a robot hand with elastic fingers. In M. Brady and et al., editors, *Robot Motion: Planning and Control*, pages 323–335, MIT Press, 1982.

[8] N. Hogan. Impedance control: an approach to manipulation. *Journal of Dynamic Systems, Measurement, and Control*, 107:1–24, March 1985.

[9] O. Khatib. Real-time obstacle avoidance for manipulators and mobile robots. *The International Journal of Robotics Research*, 5(1), 1986.

[10] O. Khatib and J. Burdick. Motion and force control of robot manipulators. In *Proceedings of the 1986 IEEE Conference on Robotics and Automation*, IEEE, San Francisco, CA, April 7-10 1986.

[11] Daniel E. Koditschek. Exact robot navigation by means of potential functions: some topological considerations. In *IEEE International Conference on Robotics and Automation*, Raleigh, North Carolina, March 31 – April 3 1987.

[12] B. Krogh. A generalized potential field approach to obstacle avoidance control. In *SME Conf. Proc. Robotics Research: The Next Five Years and Beyond*, Bethlehem, Pennsylvania, August 1984.

[13] W. S. Newman and N. Hogan. High speed control and obstacle avoidance using dynamic potential functions. In *IEEE International Conference on Robotics and Automation*, Raleigh, North Carolina, March 31 – April 3 1987.

[14] R. Volpe and P. Khosla. Artificial potentials with elliptical isopotential contours for obstacle avoidance. In *Proceedings of the 26th IEEE Conference on Decision and Control*, pages 180–185, Los Angeles, CA, December 9-11, 1987.